Acta Mechanica Solida Sinica, Vol. 27, No. 6, December, 2014 ISSN 0894-9166
Published by AMSS Press, Wuhan, China

FREE VIBRATION ANALYSIS OF FLUID-CONVEYING CARBON NANOTUBE VIA WAVE METHOD**

Zijun Zhang* **Yongshou Liu** **Baohui Li**

(*Department of Engineering Mechanics, Northwestern Polytechnical University, Xi'an* 710072, *China*)

Received 21 March 2013, revision received 23 May 2014

ABSTRACT The wave method is introduced to vibration analysis of the fluid-conveying carbon nanotube. The constitutive relation of carbon nanotube on micro-scale is founded using the non-local elastic theory. The governing equation on micro-scale is obtained. And the first five orders of the natural frequency of the carbon nanotube conveying fluid with various speeds are calculated through the wave method. Besides, the critical flow velocity when the carbon nanotube loses stability is obtained. Meanwhile, a contrast is made between the result obtained through the wave method and that in previous researches.

KEY WORDS wave method, non-local elastic theory, natural frequency, critical flow velocity

I. INTRODUCTION

The carbon nanotube (CNT) discovered by Iijima in 1991[1] as a new form of carbon element has an extremely high strength, which is a huge potential of fluid conveyance[2]. When CNTs are conveying fluid, the flow-induced vibration will occur. Many researchers have studied the flow-induced vibration of CNTs via molecular dynamics simulation or traditional elastic theory. M. Mir has simulated the vibration characteristics of various CNTs by using the finite element method[3]. Y. Yan has studied the natural frequency and the aspects that may affect the natural frequency of triple-walled CNTs[4].

As a pipe on nanometer scale, the scale effect has not been taken into consideration in the model of CNT based on the traditional elastic theory. To solve this problem, researchers resorted to non-local continuum mechanics for the research on CNT. H.M. Ma et al. have researched a microstructure-dependent Timoshenko beam model based on a modified couple stress theory[5]. L.L. Ke and Y.S. Wang have used modified couple stress theory to research the size effect on the dynamic stability of micro-beams[6]. M. Simsek has made a dynamic analysis of an embedded micro-beam carrying a moving micro-particle based on the modified couple stress theory[7]. On the other hand, G.M. Qu et al. have investigated the scattering of antiplane shear waves by two Griffith cracks using the non-local theory[8]. A.R. Setoodeh et al. have researched exact nonlocal solution for post buckling of single-walled carbon nanotubes[9]. M. Simsek and H.H. Yurtcu have obtained analytical solutions for bending and buckling of functionally graded nanobeams based on the nonlocal Timoshenko beam theory[10]. The basic idea of nonlocal continuum mechanics is that the strain state of a point refers to the stress states of all the points in the elastic body, instead of the stress state of this point alone, and this is the stress gradient

* Corresponding author. E-mail: zhangzijun@mail.nwpu.edu.cn
** The authors acknowledge the support of a grant from Aeronautical Science Foundation of China (2010ZA53013 and 2011ZA53014), the open funds of Key Laboratory of Advanced Design and Intelligent Computing(Dalian University), Ministry of Education (ADIC2010007) and Northwestern Polytechnical University Basic Research Fund(JC201114 and JC20110255), to whom the authors express their deep gratitude.

theory widely used in research[11]. Furthermore, H. Askes and E.C. Aifantis have expanded this theory to the strain gradient theory, or the so-called strain-inertia gradient theory[12]. They held that the strain state of a point also refers to the change rate of strain. D.C.C. Lam et al. have tried to validate the strain gradient elasticity by experiment[13]. S.L. Kong et al. have addressed the static and dynamic characteristics of micro beams based on the strain gradient elasticity theory[14].

There have been many researches on the dynamics of fluid conveying pipe. Q. Ni et al.[15] and Q. Qin et al.[16] have developed the differential quadrature method to tackle the chaotic transients in a curved fluid-conveying tube and the stability of upward-fluid-conveying pipe immersed in rigid cylindrical channel. L. Wang et al. have studied Hopf bifurcation of a nonlinear restrained curved pipe conveying fluid through the differential quadrature method[17]. Z.M. Wang et al.[18] and F. Zhao et al.[19] have dealt with the dynamic behaviors of viscoelastic pipe conveying fluid with the Kelvin model and three-parameter solid model, respectively. X. Jian et al. have exploited the 2-dimensional bifurcations in cantilevered pipe conveying time varying fluid[20]. But in the nanometer scale, there have been but a few researches on the dynamics of fluid-conveying tube. L. Wang et al.[21] have studied the wave propagation of fluid-conveying single-walled CNT through the strain-inertia gradient theory, and calculated the critical flow speed when CNT loses stability. Also, L. Wang et al have focused on the vibration characteristics and stability of fluid-conveying micro-pipe with scale effects[2,22].

As an analytical method of calculating the dynamic response of piping system or truss structure, the wave method has its governing equation built by analyzing the circulation transfer of the elastic wave. Reflection and transmission will occur on the boundary. B. Li et al. have used the wave method to learn more about the in-plane vibration of curved pipe and multi-span fluid conveying pipe[23,24].

In this paper, the constitutive relation of carbon nanotube in micro-scale is formed through the non-local elastic theory. Then the first five orders of the natural frequency of the fluid conveying carbon nanotubes with various speeds are calculated through the wave method. And the critical speed of fluid when the carbon nanotube loses stability is obtained, which agrees well with the result in L. Wang's research[21]. The application of the wave method in the vibration of the micro-scale pipe is rational.

II. DYNAMICS MODEL OF FLUID CONVEYING CNT

2.1. Nonlocal Continuum Mechanics Theory

In the traditional linear elastic model, the constitutive relation of an elastic object can be expressed as

$$\sigma = C\varepsilon \tag{1}$$

where C is the elastic module matrix, σ is the stress state of the point studied, and ε is the strain state of this point.

In the non-local continuum mechanics model, the strain state of one point in an elastic body refers not only to the stress state of this point, but also to the stress state of all the points in the elastic body. According to the theory of Eringen[3], the constitutive relation based on the stress gradient theory is

$$\left(1-\tau_0^2 l^2 \nabla^2\right)\sigma = C\varepsilon \tag{2}$$

In Eq.(2), $\tau_0 = e_0 a/l$ is a parameter which represents the scale effect, e_0 depends on the material. And a/l is the characteristic length ratio, where 'a' is an internal characteristic length (e.g., lattice parameter, granular distance) and l is the external characteristic length (e.g., crack length, wavelength)[7]. $a = d_0/\sqrt{12}$, where $d_0 = 1.23\times10^{-10}$ m refers to the inter-particle distance, which is the axial distance between two rings of carbon atoms for the single-walled carbon nanotube[25]. When the dimension to be researched is one, Eq.(2) can be written as

$$\left(1-\tau^2 l^2 \frac{\partial^2}{\partial x^2}\right)\sigma = E\varepsilon \tag{3}$$

Then, we can develop stress gradient theory to strain-inertia gradient theory. According to the research of Askes[12], the constitutive relation based on the strain-inertia gradient theory is

$$\sigma = E\left(1-l_1^2\frac{\partial^2}{\partial x^2}\right)\varepsilon + \rho l_2^2 \frac{\partial^2 \varepsilon}{\partial t^2} \tag{4}$$

where l_1 and l_2 are internal characteristic length values determined by experiment or microscopic models. $l_1 = a = 3.55 \times 10^{-11}$ m, $l_2/l_1 = 10$ for (20,20) CNT[12]. Actually, l_1 and l_2 show the importance of the change rate of strain with respect to position and time ($\partial^2\varepsilon/\partial x^2$ and $\partial^2\varepsilon/\partial t^2$), respectively.

2.2. Timoshenko Beam Model of CNT

As shown in Fig.1, a model of fluid-conveying CNT with fixed constraints at both ends is built. By analyzing the stress on the cross-section, the bending moment can be obtained.

$$M = \int_A \sigma y \mathrm{d}A \tag{5}$$

Substituting Eq.(4) into Eq.(5), we have

$$M = -EI\left(\frac{\partial^2 w}{\partial x^2} - l_1^2\frac{\partial^4 w}{\partial x^4}\right) - \rho I l_2^2 \frac{\partial^4 w}{\partial x^2 \partial t^2} \tag{6}$$

where w is the deflection of the CNT, and $I = \int_A y^2 \mathrm{d}A$ represents the moment of inertia for the cross section.

Then the dynamic differential equation of the fluid-conveying CNT can be obtained as

$$\frac{\partial F}{\partial x} - \rho_f A_f\left(\frac{\partial^2 w}{\partial t^2} + 2U\frac{\partial^2 w}{\partial x \partial t} + U^2\frac{\partial^2 w}{\partial x^2}\right) = \rho_t A_t \frac{\partial^2 w}{\partial t^2} \tag{7}$$

where F is the shear force on the cross-section, U is the mean flow velocity of the fluid[26]. In this paper, fluid is considered incompressible. According to the research of L. Wang[26], the fluid conveyed in nanotube cannot permeate the pipe wall because the length of the C-C bond is far smaller than the diameter of the fluid molecule. According to the research of Tuzun[27], the friction force between fluid and pipe wall can be neglected because the friction force is far smaller than the Coriolis force caused by the fluid. As the same reason, plug flow assumption is introduced into the research on CNT conveying fluid. The relationship between F and the bending moment M is

$$F = \frac{\partial M}{\partial x} + \rho I \frac{\partial^2 \Phi}{\partial t^2} \tag{8}$$

where Φ is the curvature ratio caused by bending moment. Shear stress and strain must be taken into consideration in Timoshenko beam model. The constitutive relation between shear stress and strain is

$$\tau = G\left(1 - l_1^2\frac{\partial^2}{\partial x^2}\right)\gamma + \rho l_2^2 \frac{\partial^2 \gamma}{\partial t^2} \tag{9}$$

Then the shear force F can be represented as

$$F = \int_A \tau \mathrm{d}A \tag{10}$$

The whole curvature ratio of the beam is

$$\frac{\partial w}{\partial x} = \Phi + \gamma \tag{11}$$

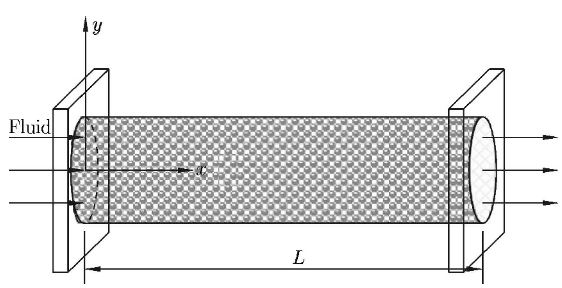

Fig. 1. CNT model with fixed constraints at both ends[26].

Substituting Eq.(11) into Eq.(6) and equation Eq.(10), respectively, we can conclude,

$$M = -EI\left(\frac{\partial \Phi}{\partial x} - l_1^2\frac{\partial^3 w}{\partial x^3}\right) - \rho I l_2^2 \frac{\partial^5 w}{\partial x^3 \partial t^2} \tag{12}$$

$$F = GA_t k\left[\frac{\partial w}{\partial x} - \Phi - l_1^2\left(\frac{\partial^3 w}{\partial x^3} - \frac{\partial^2 \Phi}{\partial x^2}\right)\right] + \rho A_t k l_2^2\left(\frac{\partial^3 w}{\partial x \partial t^2} - \frac{\partial^2 \Phi}{\partial t^2}\right) \tag{13}$$

where k is the shear coefficient of CNT, for the thin-walled circular pipe, k is equal to $2(1+\nu)/(4+3\nu)$. Then substituting Eqs.(12) and (13) into Eq.(7), the governing equation of bending can be obtained.

$$\begin{aligned} &GA_t k\left(\frac{\partial^2 w}{\partial x^2} - \frac{\partial \Phi}{\partial x} - l_1^2\frac{\partial^4 w}{\partial x^4} + l_1^2\frac{\partial^3 \Phi}{\partial x^3}\right) + \rho_t A_t k l_2^2\left(\frac{\partial^4 w}{\partial x^2 \partial t^2} - \frac{\partial^3 \Phi}{\partial x \partial t^2}\right) \\ &-\rho_f A_f\left(U^2\frac{\partial^2 w}{\partial x^2} + 2U\frac{\partial^2 w}{\partial x \partial t} + \frac{\partial^2 w}{\partial t^2}\right) - \rho_t A_t\frac{\partial^2 w}{\partial t^2} = 0 \end{aligned} \tag{14}$$

The differential equation of the torsion motion of Timoshenko beam can be represented as

$$F - \frac{\partial M}{\partial x} = (J_t + J_f)\frac{\partial^2 \Phi}{\partial t^2} \tag{15}$$

where J_t and J_f are the moment of inertia of the CNT and the fluid, respectively. Substituting Eqs.(12) and (13) into Eq.(15), we conclude,

$$\begin{aligned} &EI\left(\frac{\partial^2 w}{\partial x^2} - l_1^2\frac{\partial^4 w}{\partial x^4}\right) + \rho_t I l_2^2\frac{\partial^4 \Phi}{\partial x^2 \partial t^2} + GA_t k\left(\frac{\partial w}{\partial x} - \Phi - l_1^2\frac{\partial^3 w}{\partial x^3} + l_1^2\frac{\partial^2 \Phi}{\partial x^2}\right) \\ &+\rho_t A_t k l_2^2\left(\frac{\partial^3 w}{\partial x \partial t^2} - \frac{\partial^2 \Phi}{\partial t^2}\right) - (J_t + J_f)\frac{\partial^2 \Phi}{\partial t^2} = 0 \end{aligned} \tag{16}$$

Equations (14) and (16) are the governing equations of the fluid-structure interaction[21].

III. VIBRATION ANALYSES THROUGH WAVE METHOD

3.1. Wave Method Used in Fluid-conveying CNT Vibration Analysis

The elastic wave in a pipe can be regarded as vibration propagation in the pipe. Given that the vibration of the pipe can be resolved into several simple harmonic vibrations, the elastic wave in the pipe can be regarded as a superposition of several harmonic waves. The harmonic wave components can be represented as Eqs.(17).

$$w(x,t) = W\exp\left[\mathrm{i}\kappa(x-ct)\right], \quad \phi(x,t) = \varphi\exp\left[\mathrm{i}\kappa(x-ct)\right] \tag{17}$$

where $\mathrm{i} = \sqrt{-1}$. Substituting Eqs.(17) into Eqs.(14) and Eq.(16), we conclude that

$$\begin{aligned} &W\left[-GA_t k\kappa^2\left(1+l_1^2\kappa^2\right) + \rho_t A_t k l_2^2\kappa^4 c^2 + \rho_f A_f U^2\kappa^2 - 2\rho_f A_f U\kappa^2 c + (\rho_f A_f + \rho_t A_t)\kappa^2 c^2\right] \\ &\quad = \mathrm{i}\kappa\varphi\left[GA_t k\left(1+l_1^2\kappa^2\right) - \rho_t A_t k l_2^2\kappa^2 c^2\right] \\ &W\left[\kappa^2 GA_t k\left(1+l_1^2\kappa^2\right) - \rho_t A_t k l_2^2\kappa^4 c^2\right] \\ &\quad = \mathrm{i}\kappa\varphi\left\{-GA_t k\left(1+l_1^2\kappa^2\right) + \kappa^2 c^2\left[(J_t+J_f) + \rho_t A_t k l_2^2 + \rho_t I_t l_2^2\kappa^2\right] - \kappa^2 EI_t\left(1+l_1^2\kappa^2\right)\right\} \end{aligned} \tag{18}$$

Then the dispersion equation of the wave in CNT can be obtained as follows:

$$\begin{aligned} &\left[-GA_t k\left(1+l_1^2\kappa^2\right) + \rho_t A_t l_2^2\kappa^2 c^2 + \rho_f A_f U^2 - 2\rho_f A_f U c + (\rho_f A_f + \rho_t A_t)c^2\right] \\ &\quad \times\left\{-GA_t k\left(1+l_1^2\kappa^2\right) + \kappa^2 c^2\left[(J_t+J_f) + \rho_t A_t k l_2^2 + \rho_t I_t l_2^2\kappa^2\right] - \kappa^2 EI_t\left(1+l_1^2\kappa^2\right)\right\} \\ &\quad = \left[GA_t k\left(1+l_1^2\kappa^2\right) - \rho_t A_t k l_2^2\kappa^2 c^2\right]^2 \end{aligned} \tag{19}$$

The dispersion equation with respect to κ has eight roots, two of which are real roots corresponding to travel waves while the remaining six are conjugate complex numbers corresponding to the gradually

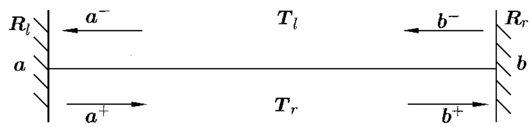

Fig. 2. Wave propagation in CNT.

failing waves. Consider the direction along the pipe axis only, and let $\kappa_{1,2,3,4}$ and $\kappa_{5,6,7,8}$ represent wave numbers of the right- and left-travelling waves, respectively. Given that κ_1 and κ_5 are the two real roots, then the other six can be expressed as $\kappa_2 = \overline{\kappa_6}$, $\kappa_3 = \overline{\kappa_7}$, $\kappa_4 = \overline{\kappa_8}$ respectively.

The wave propagating in CNT is a superposition of the eight waves above.

$$w(x,t) = \sum_{j=1}^{8} C_{wj} \exp\left[\mathrm{i}\left(\kappa_j x - \omega t\right)\right], \quad \phi(x,t) = \sum_{j=1}^{8} C_{\phi j} \exp\left[\mathrm{i}\left(\kappa_j x - \omega t\right)\right] \tag{20}$$

The transfer of the elastic wave in CNT is reflected at the boundaries. As shown in Fig.2, $\boldsymbol{a}$ and $\boldsymbol{b}$ represent the vibrations at the ends of CNT. Given that $\boldsymbol{a}$ and $\boldsymbol{b}$ are expressed as $\boldsymbol{a} = \{a_1, a_2, a_3, a_4, a_5, a_6, a_7, a_8\}^{\mathrm{T}}$ and $\boldsymbol{b} = \{b_1, b_2, b_3, b_4, b_5, b_6, b_7, b_8\}^{\mathrm{T}}$, respectively, and setting $\boldsymbol{a}^- = \{a_1, a_2, a_3, a_4\}^{\mathrm{T}}$, $\boldsymbol{b}^- = \{b_1, b_2, b_3, b_4\}^{\mathrm{T}}$, $\boldsymbol{a}^+ = \{a_5, a_6, a_7, a_8\}^{\mathrm{T}}$, $\boldsymbol{b}^+ = \{b_5, b_6, b_7, b_8\}^{\mathrm{T}}$,the propagation and reflection of wave in CNT can be illustrated by Eqs.(21) and Eq.(22).

$$\boldsymbol{a}^- = \boldsymbol{T}_l \boldsymbol{b}^-, \quad \boldsymbol{b}^+ = \boldsymbol{T}_r \boldsymbol{a}^+ \tag{21}$$

$$\boldsymbol{a}^+ = \boldsymbol{R}_l \boldsymbol{a}^-, \quad \boldsymbol{b}^- = \boldsymbol{R}_r \boldsymbol{b}^+ \tag{22}$$

Then the propagation matrix of the wave in CNT can be derived from Eq.(20), that is,

$$\begin{gathered}\boldsymbol{T}_l = \begin{bmatrix} \exp(-\mathrm{i}\kappa_1 L) & 0 & 0 & 0 \\ 0 & \exp(-\mathrm{i}\kappa_2 L) & 0 & 0 \\ 0 & 0 & \exp(-\mathrm{i}\kappa_3 L) & 0 \\ 0 & 0 & 0 & \exp(-\mathrm{i}\kappa_4 L) \end{bmatrix} \\ \boldsymbol{T}_r = \begin{bmatrix} \exp(\mathrm{i}\kappa_5 L) & 0 & 0 & 0 \\ 0 & \exp(\mathrm{i}\kappa_6 L) & 0 & 0 \\ 0 & 0 & \exp(\mathrm{i}\kappa_7 L) & 0 \\ 0 & 0 & 0 & \exp(\mathrm{i}\kappa_8 L) \end{bmatrix}\end{gathered} \tag{23}$$

where L is the length of the CNT. The reflection matrix of the wave at the boundaries can be derived from the boundary conditions. The boundary conditions of the fixed CNT can be expressed as

$$w|_{x=0} = 0, \quad w|_{x=L} = 0, \quad \Phi|_{x=0} = 0, \quad \Phi|_{x=L} = 0, \quad \gamma|_{x=0} = 0, \quad \gamma|_{x=L} = 0 \tag{24}$$

Meanwhile, Eqs.(24) can be written as Eqs.(25).

$$\begin{gathered}\sum_{j=1}^{8} C_{wj} = 0, \quad \sum_{j=1}^{8} C_{wj} \exp(\mathrm{i}\kappa_j L) = 0 \\ \sum_{j=1}^{8} C_{\Phi j} = 0, \quad \sum_{j=1}^{8} C_{\Phi j} \exp(\mathrm{i}\kappa_j L) = 0 \\ \sum_{j=1}^{8} \kappa_j C_{wj} = 0, \quad \sum_{j=1}^{8} \kappa_j C_{wj} \exp(\mathrm{i}\kappa_j L) = 0\end{gathered} \tag{25}$$

According to Eqs.(18), the relation between C_{wj} and $C_{\Phi j}$ can be obtained as Eq.(26).

$$C_{wj} = \zeta_j C_{\Phi j} \tag{26}$$

where,

$$\zeta_j = \frac{\mathrm{i}\kappa_j \left[GA_t k\left(1 + l_1^2 \kappa_j^2\right) - \rho_t A_t k l_2^2 \kappa_j^2 c^2\right]}{-GA_t k \kappa_j^2 \left(1 + l_1^2 \kappa_j^2\right) + \rho_t A_t k l_2^2 \kappa_j^4 c^2 + \rho_f A_f U^2 \kappa_j^2 - 2\rho_f A_f U \kappa_j^2 c + \left(\rho_f A_f + \rho_t A_t\right) \kappa_j^2 c^2} \quad (j = 1, 2, \ldots 8) \tag{27}$$

According to Eqs.(25)-(27), the reflection matrix of wave at the boundaries can be selected as follows:

$$\boldsymbol{R}_l = -\begin{bmatrix} 1 & 1 & 1 & 1 \\ \zeta_5 & \zeta_6 & \zeta_7 & \zeta_8 \\ \kappa_5 & \kappa_6 & \kappa_7 & \kappa_8 \\ \mathrm{e}^{\mathrm{i}\kappa_5 L} & \mathrm{e}^{\mathrm{i}\kappa_6 L} & \mathrm{e}^{\mathrm{i}\kappa_7 L} & \mathrm{e}^{\mathrm{i}\kappa_8 L} \end{bmatrix}^{-1} \begin{bmatrix} 1 & 1 & 1 & 1 \\ \zeta_1 & \zeta_2 & \zeta_3 & \zeta_4 \\ \kappa_1 & \kappa_2 & \kappa_3 & \kappa_4 \\ \mathrm{e}^{\mathrm{i}\kappa_1 L} & \mathrm{e}^{\mathrm{i}\kappa_2 L} & \mathrm{e}^{\mathrm{i}\kappa_3 L} & \mathrm{e}^{\mathrm{i}\kappa_4 L} \end{bmatrix} \tag{28a}$$

$$\boldsymbol{R}_r = -\begin{bmatrix} 1 & 1 & 1 & 1 \\ \zeta_1 & \zeta_2 & \zeta_3 & \zeta_4 \\ \kappa_1 & \kappa_2 & \kappa_3 & \kappa_4 \\ \mathrm{e}^{-\mathrm{i}\kappa_1 L} & \mathrm{e}^{-\mathrm{i}\kappa_2 L} & \mathrm{e}^{-\mathrm{i}\kappa_3 L} & \mathrm{e}^{-\mathrm{i}\kappa_4 L} \end{bmatrix}^{-1} \begin{bmatrix} 1 & 1 & 1 & 1 \\ \zeta_5 & \zeta_6 & \zeta_7 & \zeta_8 \\ \kappa_5 & \kappa_6 & \kappa_7 & \kappa_8 \\ \mathrm{e}^{-\mathrm{i}\kappa_5 L} & \mathrm{e}^{-\mathrm{i}\kappa_6 L} & \mathrm{e}^{-\mathrm{i}\kappa_7 L} & \mathrm{e}^{-\mathrm{i}\kappa_8 L} \end{bmatrix} \tag{28b}$$

3.2. Discussion on the Wave Method

The reflection of wave at the boundary of CNT determines the reflection matrix. A wave circulation is formed in the fixed CNT, as illustrated in Fig.2. Actually, without considering the energy dissipation as a constraint, the energy in the elastic wave will not decrease. Since the elastic modulus of CNT can be as high as 1 TPa, the dispersion during transfer can be neglected.

The order of the reflection matrix refers to the number of roots of the dispersion equation. On the other hand, the reflection matrix is derived from the boundary conditions. For statically determinate problems, the order of the reflection matrices based on the two methods above will be identical. But to statically indeterminate problems, the order of reflection matrices derived from the dispersion equation and the boundary conditions will not be identical. In this paper, a Timoshenko beam model fixed at both ends is used, so the problem is a statically indeterminate problem. A simplification of the boundary conditions is made by applying Sanit Venant principle.

As the wave transfers circularly in the CNT, by combining Eqs.(21) and (22), we conclude that

$$\boldsymbol{a}^+ = \boldsymbol{R}_l \boldsymbol{a}^- = \boldsymbol{R}_l \boldsymbol{T}_l \boldsymbol{b}^- = \boldsymbol{R}_l \boldsymbol{T}_l \boldsymbol{R}_r \boldsymbol{b}^+ = \boldsymbol{R}_l \boldsymbol{T}_l \boldsymbol{R}_r \boldsymbol{T}_r \boldsymbol{a}^+ = \boldsymbol{A}\boldsymbol{a}^+ \tag{29}$$

i.e. ,

$$(\boldsymbol{I} - \boldsymbol{A})\,\boldsymbol{a}^+ = 0 \tag{30}$$

And, only when Eq.(31) is valid will Eq.(30) have nontrivial solutions.

$$H(\omega) = \det H(\omega) = \det(\boldsymbol{I} - \boldsymbol{A}) = 0 \tag{31}$$

Equation (31) is the characteristic equation of the wave method. Considering that $c = \omega/\kappa$, where ω is the wave frequency and κ is the wave number, we can conclude that the only unknown quantity in Eq.(31) is ω. The solution of Eq.(31) for ω is the natural frequency of the fluid-conveying CNT.

The displacement shape function is replaced by the wave solution of the governing equation in the wave method. So the wave method is an analytical method which is more accurate than the numerical method. Meanwhile, the number of wave modes in actual problems is small, so the efficiency of computation is high. But when the dispersion equation is complex, the wave solution of the dispersion equation can only be obtained via the numerical method. So error will accumulate in the following calculation. Nevertheless, the wave method is meaningful in theoretical analysis.

IV. CALCULATION AND DISCUSSION

4.1. The Natural Frequency of CNT Based on Strain-inertia Gradient Theory

There are two scale effect parameters in the constitutive equation based on the strain-inertia gradient theory. Take the CNT with form (20, 20) for example, the scale effect parameters are $l_1 = 3.55 \times 10^{-11}$ m, $l_2/l_1 = 10$ respectively[12]. For single-walled CNTs, the density is $\rho_t = 2.3 \times 10^3$ kg/m^3, the elasticity modulus is $E = 1.27$ TPa, and the Poisson's ratio is $\nu = 0.2$. The thickness of the wall is $\delta = 3.4 \times 10^{-10}$ m[25], the outer diameter of CNT is chosen as $D = 1.4 \times 10^{-8}$ m. The moment of inertia for the cross section is $I = \dfrac{\pi}{64}(D^4 - d^4)$. The rotational inertia of CNT and that of the fluid are $J_t = \dfrac{1}{4}\rho_t A_t \left[\left(\dfrac{D}{2}\right)^2 + \left(\dfrac{d}{2}\right)^2\right]$, $J_f = \dfrac{1}{4}\rho_f A_f \left(\dfrac{d}{2}\right)^2$, respectively.

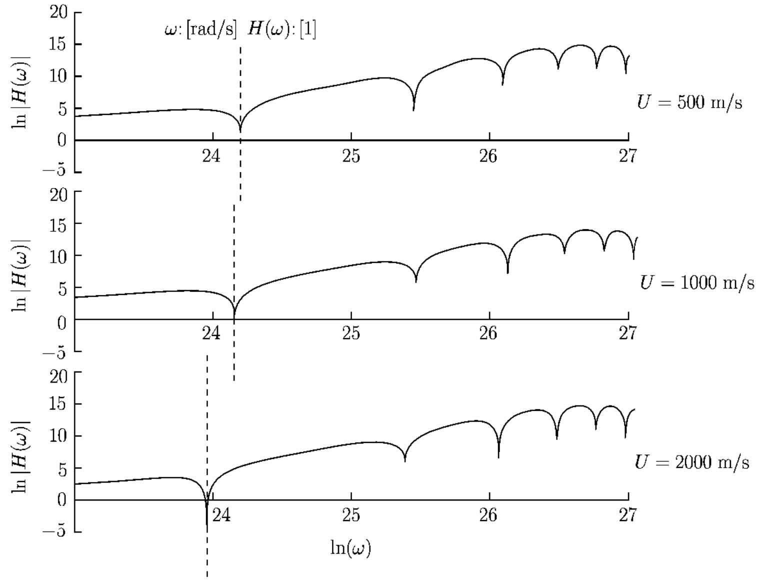

Fig. 3. The curve of $\ln|H(\omega)|$ with respect to $\ln(\omega)$ under different fluid velocities.

The step length of $\ln(\omega)$ is chosen as 1.0×10^{-3}, and the curve of $\ln|H(\omega)|$ with respect to $\ln(\omega)$ can be obtained for different flow velocities.

As shown in Eq.(31), the solution of the equation must guarantee that the real part and the imaginary part of the determinant are both equal to zero. The relative points are hard to find directly. So $\ln|H(\omega)|$ is employed as the vertical axis. When the determinant of $H(\omega)$ equals zero, $\ln|H(\omega)|$ tends to be negative infinity. So the curve presents a 'sharp tip', as shown in Fig.3. The abscissa values relative to the 'sharp tips' are the approximate values of the natural frequencies.

The first five orders of the natural frequency of fluid conveying CNT with various speeds are obtained through the same procedure as mentioned above.

Table 1. **The first five orders of the natural frequency of fluid conveying CNT**

U (m/s)	1st to 5th order natural frequency ($\times10^{10}$rad/s)				
0	3.908	11.848	22.078	32.618	42.938
500	3.870	11.801	22.071	32.413	42.938
1000	3.721	11.737	21.868	32.294	42.515
2000	3.200	10.988	20.832	31.056	40.872
2500	2.724	10.485	20.045	29.868	39.686
3000	1.990	9.731	19.093	28.717	38.153

Natural frequencies decrease with an increase of fluid velocity, as shown in Fig.3 and Table 1. When the fluid velocity is sufficiently great, the first-order natural frequency will vanish. The critical velocity when zero natural frequency appears is related to the instability of CNT. Through further calculation, the curve of the first-order frequency with respect to fluid velocity can be obtained, as shown in Fig.4.

By choosing the step length of fluid velocity as 25 m/s, the critical flow velocity related to the instability of CNT can be obtained as 3875 m/s for the strain gradient Timoshenko beam model.

For the purpose of contrast, the natural frequency of CNT based on the stress gradient theory is calculated. According to Eq.(2) and the process derived in this paper, the first-order natural frequencies of CNT with various flow speeds are obtained, as shown in Fig.4.

4.2. Contrasts and Discussions

In Wang's research[21] the curve of phase velocity with respect to the flow velocity for strain-inertia and the stress gradient Timoshenko beam model is as follows.

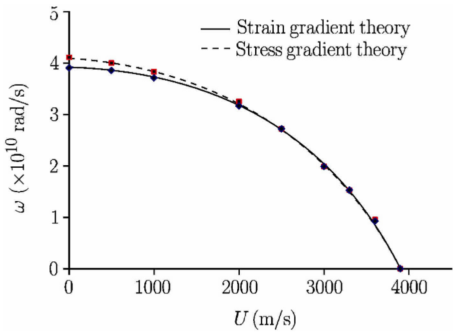

Fig. 4. The curve of 1st order frequency with respect to fluid velocity.

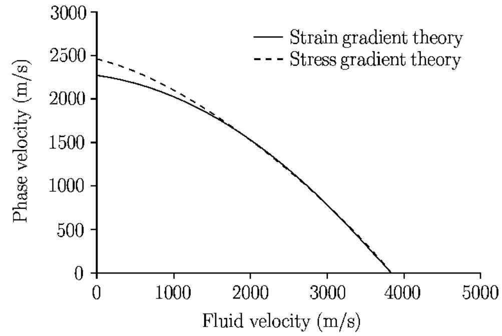

Fig. 5. Phase velocity of CNT versus fluid speed[21].

The trends of Fig.4 are similar to those in Fig.5. Considering the relation between frequency and phase velocity, i.e. $c = \omega/\kappa$, the similarity of the trends can be proved.

According to Fig.4, the critical flow speed based on strain-inertia gradient theory and that on stress gradient theory are 3875 m/s and 3900 m/s, respectively. Contrasts between the results in this paper and in previous research are listed in Table 2.

Table 2. **Contrast of critical velocities**

	Strain gradient theory	Stress gradient theory
This paper	3875 m/s	3900 m/s
Wang's research[21]	3850 m/s	3850 m/s
Relative error	$< 0.65\%$	$< 1.30\%$

As shown in Table 2, the results in this paper agree well with those in Wang's research[21]. However, the calculated results in this paper have a certain degree of error as the step length of ω should not be too small to guarantee the efficiency of calculation.

V. SUMMARY

The vibration characteristics of fluid-conveying CNT are researched in this paper based on the non-local continuum mechanics theory. The first five orders of natural frequency of the fluid-conveying CNT are calculated with the wave method. Meanwhile, the critical flow speed when CNT loses stability is found to be 3875 m/s for strain gradient Timoshenko beam model.

For the purpose of contrast, the critical flow speed is calculated based on stress gradient theory. The result 3900 m/s is bigger than the result via strain-inertia theory.

These results are in agreement with those in Ref.[21]. The analysis and contrast mentioned above prove that it is rational to use the wave method in the vibration analysis of fluid-conveying CNT. This provides a new thought in the research on mirco-pipe dynamics.

References

[1] Iijima,S., Helical microtubules of graphitic carbon. *Nature*, 1991, 354(6348): 56-58.
[2] Wang,L., Ni,Q. and Li,M., Buckling instability of double-walled fluid conveying carbon nanotubes. *Computational Materials Science*, 2008, 44(2): 821-825.
[3] Mir,M., Hosseini,A. and Majzoobi,G.H., A numerical study of vibrational properties of single-walled carbon nanotubes. *Computational Materials Science*, 2008, 43(3): 540-548.
[4] Yan,Y., He,X.Q., Zhang,L.X. and Wang,C.M., Dynamic behavior of triple-walled fluid conveying carbon nanotubes. *Journal of Sound and Vibration*, 2009, 319(3-5): 1003-1018.
[5] Ma,H.M., Gao,X.L. and Reddy,J.N., A microstructure-dependent Timoshenko beam model based on a modified couple stress theory. *Journal of the Mechanics and Physics of Solids*, 2008, 56(12): 3379-3391.
[6] Ke,L.L. and Wang,Y.S., Size effect on dynamic stability of functionally graded microbeams based on a modified couple stress theory. *Composite Structures*, 2011, 93(2): 342-350.

[7] Simsek,M., Dynamic analysis of an embedded microbeam carrying a moving microparticle based on the modified couple stress theory. *International Journal of Engineering Science*, 2010, 48(12): 1721-1732.

[8] Qu,G.M., Zhou,Z.G. and Du,S.Y., Investigation of the scattering of antiplane shear waves by two Griffith cracks using the non-local theory. *Acta Mechanica Solida Sinica*, 1999, 12(3): 211-219.

[9] Setoodeh,A.R., Khosrownejad,M. and Malekzadeh,P., Exact nonlocal solution for postbuckling of single-walled carbon nanotubes. *Physica E-Low-Dimensional Systems* & *Nanostructures*, 2011, 43(9): 1730-1737.

[10] Simsek,M. and Yurtcu,H.H., Analytical solutions for bending and buckling of functionally graded nanobeams based on the nonlocal Timoshenko beam theory. *Composite Structures*, 2013, 97: 378-386.

[11] Eringen,A.C., On differential-equations of nonlocal elasticity and solutions of screw dislocation and surface-waves. *Journal of Applied Physics*, 1983, 54(9): 4703-4710.

[12] Askes,H. and Aifantis,E.C., Gradient elasticity and flexural wave dispersion in carbon nanotubes. *Physical Review B*, 2009, 80(19): 1-8.

[13] Lam,D.C.C., Yang,F., Chong,A.C.M., Wang,J. and Tong,P., Experiments and theory in strain gradient elasticity. *Journal of the Mechanics and Physics of Solids*, 2003, 51(8): 1477-1508.

[14] Kong,S., Zhou,S., Nie,Z. and Wang,K., Static and dynamic analysis of micro beams based on strain gradient elasticity theory. *International Journal of Engineering Science*, 2009, 47(4): 487-498.

[15] Ni,Q., Wang,L. and Qian,Q., Chaotic transients in a curved fluid conveying tube. *Acta Mechanica Solida Sinica*, 2005, 18(3): 207-214.

[16] Qian,Q., Wang,L. and Ni,Q., Vibration and stability of vertical upward-fluid-conveying pipe immersed in rigid cylindrical channel. *Acta Mechanica Solida Sinica*, 2008, 21(5): 431-440.

[17] Wang,L., Ni,Q. and Huang,Y.Y., Hopf bifurcation of a nonlinearly restrained fluid conveying curved pipe by differential quadrature method. *Acta Mechanica Solida Sinica*, 2003, 16(4): 345-352.

[18] Wang,Z.M., Zhao,F.Q., Feng,Z.Y. and Liu,H.Z., The dynamic behaviors of viscoelastic pipe conveying fluid with the Kelvin model. *Acta Mechanica Solida Sinica*, 2000, 13(3): 262-270.

[19] Zhao,F., Wang,Z. and Feng,Z., Analysis of the dynamic behaviors of viscoelastic pipe conveying fluid with three-parameter solid model. *Acta Mechanica Solida Sinica*, 2002, 23(4): 483-489.

[20] Jian,X., Wai,C.K. and Ying,C.H.S., Co-dimension 2 bifurcations and chaos in cantilevered pipe conveying time varying fluid with three-to-one internal resonances. *Acta Mechanica Solida Sinica*, 2003, 16(3): 245-255.

[21] Wang,L., Wave propagation of fluid-conveying single-walled carbon nanotubes via gradient elasticity theory. *Computational Materials Science*, 2010, 49(4): 761-766.

[22] Wang,L., Vibration and instability analysis of tubular nano- and micro-beams conveying fluid using nonlocal elastic theory. *Physica E-Low-Dimensional Systems* & *Nanostructures*, 2009, 41(10): 1835-1840.

[23] Li,B., Gao,H., Liu,Y., Lu,H. and Yue,Z., Wave propagation method for in-plane vibration of curved pipe conveying fluid. *Acta Mechanica Solida Sinica*, 2012, 33(3): 302-308.

[24] Li,B., Gao,H., Zhai,H., Liu,Y. and Yue,Z., Free vibration analysis of multi-span pipe conveying fluid with dynamic stiffness method. *Nuclear Engineering and Design*, 2011, 241(3): 666-671.

[25] Wang,L. and Hu,H., Flexural wave propagation in single-walled carbon nanotubes. *Physical Review B*, 2005, 71(19): 195412.

[26] Chang,W.J. and Lee,H.L., Free vibration of a single-walled carbon nanotube containing a fluid flow using the Timoshenko beam model. *Physics Letters A*, 2009, 373(10): 982-985.

[27] Tuzun,R.E., Noid,D.W., Sumpter,B.G. and Merkle,R.C., Dynamics of fluid flow inside carbon nanotubes. *Nanotechnology*, 1996, 7(3): 241.